The Effect of Topography on Quasi-Geostrophic Frontogenesis①

Zhao Ming (赵 鸣)
Department of Atmospheric Sciences, Nanjing University, Nanjing
Received December 22, 1989; revised April 22, 1990

ABSTRACT

This paper improves Bannon's work on the quasi-geostrophic frontogenesis in a horizontal deformation field. By setting the lower boundary condition for the equation of potential temperature on the realistic topography instead of on $z = 0$, a general solution for the temperature field is derived after applying conformal mapping to the equation for the potential temperature, the vertical velocity and divergence field are also calculated. The general characteristics for the frontogenetic process still are frontolytic for warm front and frontogenetic for cold front in downstream of a mountain and the reverse is true upstream of a mountain, but more fine spatial structure of the temperature field and frontogenetic characteristics than Bannon's are obtained near surface because of the treatment of lower boundary condition. It is concluded that the frontogenetic characteristics are related to the translating speed of the deformation field with respect to the topography.

I. INTRODUCTION

The application of deformation field to the research of frotogenesis has been made some achievements. The typical work about quasi-geostrophic model (William and Plotkin, 1968) and semi-geostrophic model (Hoskins and Bretherton, 1972) showed that a front could be formed in a horizontal deformation field. Bannon (1983,1984) had investigated the effect of topography on the frontogenesis, his first work using the quasi-geostrophic modeland found some typical conclusions, the quasi-geostrophic model which can show the main dynamic process of the effect of the topography on the frontogenesis was not satisfactory because the advection due to ageostrophic wind was not included. Bannon (1984)'s semi-geostrophic model considered the effect of ageostrophic wind, however, the effect of the topography could not be studied on a fixed geometric form of the topography on account of semi-geostrophic coordinate transformation. It seems that a systemetic and definite conclusion about the effect of the topography on the strength of a front still is lacking from synoptic meteorological analysis, because there are no enough observations in the mountain area, hence, the importance of theoretical research in this field is obvious.

In order to solve the problem conveniently, a linear approximation in the lower boundary condition had been applied in Bannon's quasi-geostrophic model, i.e., the lower boundary condition was not set at the level of topography, but at $z = 0$, therefore, the frontogenesis characteristics near the mountain level and surface could not be demonstrated obviously. This paper improves Bannon's quasi-geostrophic work by putting the lower boundary condition at the level of the topography and more general results are derived.

①This work was supported by the National Natural Science Foundation of China.

II. THE BASIC MODEL

Similar to Bannon (1983), the nondimensional adiabatic quasi-geostrophic potential vorticity equation in the f plane can be written as:

$$\frac{d}{dt}\left[\nabla^2\psi+\frac{1}{\rho_s}\frac{\partial}{\partial z}\left(\frac{\rho_s}{S}\frac{\partial\psi}{\partial z}\right)\right]=0 \tag{1}$$

where ∇^2 is horizontal Laplace operator, ψ the geostrophic streamfunction, ρ_s the environmental density, $S\equiv\frac{N^2D^2}{f^2L^2}$ the Burger number, N the Brunt frequency, D and L, the scales of depth and length respectively,

$$\frac{d}{dt}\equiv\frac{\partial}{\partial t}+u_0\frac{\partial}{\partial x}+v_0\frac{\partial}{\partial y} \tag{2}$$

and we have:

$$u_0=-\frac{\partial\psi}{\partial z},\qquad v_0=\frac{\partial\psi}{\partial x} \tag{3}$$

$$\theta=\frac{\partial\psi}{\partial z} \tag{4}$$

$$w_1=-\frac{1}{S}\frac{d\theta}{dt} \tag{5}$$

θ is the zeroth order term in the expansion of the nondimensional deviation of the potential temperature from a stably stratified basic state value Θ_0 according to εF, where ε is Rossby number, $F=\frac{f^2L^2}{gD}$ (Pedlosky,1979), w_1 is the first order term in the expansion of vertical velocity w according to ε.

The w caused by the topography may be written as (Pedlosky,1979)

$$w_1=\frac{d}{dt}\left(\frac{h_B}{\varepsilon D}\right)\qquad\text{at}\quad z=\frac{h_B}{D} \tag{6}$$

where h_B is the dimensional height of the topography. We only research two-dimensional problem and set $\frac{h_B}{D}\equiv h(x,t)$, here h_B is taken as a function of time t because deformation field has been assumed to be motionless when it moves with respect to the topography. In this paper, $\varepsilon=0.3$, $D=10$ km, $L=10^3$ km, $f=10^{-4}$ s^{-1} and $U\sim V=30$ m/s. We put

$$\psi(x,y,z,t)=\psi_0(x,y)+\varphi(x,z,t)$$

$\psi_0=\alpha xy$ is the horizontal deformation field which is independent of time, α the strength of the deformation field. Neglecting the variation of ρ_s with height, we may write Eq.(1) as:

$$\left(\frac{\partial}{\partial t}-\alpha x\frac{\partial}{\partial x}\right)\left(\frac{\partial^2\theta}{\partial x^2}+\frac{1}{S}\frac{\partial^2\theta}{\partial z^2}\right)=0 \tag{8}$$

Setting $S=1$ (corresponding to $\frac{\partial \Theta_0}{\partial z}=0.3°C/100$ m), we obtain the lower boundary condition from (5),(6),(8) as follows:

$$\left(\frac{\partial}{\partial k}-\alpha x\frac{\partial}{\partial x}\right)\left(\theta+\frac{h}{\varepsilon}\right)=0 \qquad \text{where} \quad z=\frac{h_B}{D} \tag{9}$$

The upper and lower boundary conditions are that θ is finite where $z\to\infty$ and $|x|\to\infty$.

Similar to Bannon (1983), the initial value of θ is taken as:

$$\theta(x,z,0)=F(x) \tag{10}$$

From (8), we have:

$$\frac{\partial^2\theta}{\partial x^2}+\frac{\partial^2\theta}{\partial z^2}=\left.\frac{d^2F(x)}{dx^2}\right|_{xe^{\alpha t}} \tag{11}$$

The lower boundary condition has the form:

$$\theta(x,h,t)=F(xe^{\alpha t})+\frac{1}{\varepsilon}(h[xe^{\alpha t},0)-h(x,t)] \tag{12}$$

Bannon (1983) set the lower boundary condition (13) at $z=0$, this treatment could not demonstrate the situation near the mountain. This paper improves this treatment, set the lower boundary condition at $z=h$, then the effects of blocking, strengthening or weakening of the topography on the front can be described more obviously. Bannon's treatment could simplify the procedure for finding an analytic solution, but his solution was not accurate between $z=0$ and $z=h$, which will be solved in this paper. Because the lower boundary is curvilinear, we shall use conformal mapping to transfer the curvilinear boundary into straight boundary, then solve Poisson equation (11), the solution with curvilinear lower boundary can be obtained through transformation of variables from the analytic solution with the straight lower boundary. In order to simplify the problem, assuming that the shape of the mountain is semi-circular in the above mentioned nondimensionl coordinate system, i.e.,

$$\begin{aligned} &h=\sqrt{r^2-x^2} && \text{for} \quad |x|\leqslant r \\ &h=0 && \text{for other} \quad x \end{aligned} \tag{13}$$

where r is the radius of the semi-circle, and the center of the semi-circle is located at the center of the deformation field. At first, we shall assume that the mountain will not remove its location with respect to the deformation field, later, we shall consider the situations that the center of the mountain is not located at the center of the deformation field and that the mountain moves with respect to the latter by coordinate transformation.

Assuming that the conformal mapping

$$\zeta+i\eta\equiv W=\Phi(Z)=\Phi(x+iz) \tag{14}$$

can transform the semi-circle convex and the real axis outside the semi-circle in the Z-plane into the real axis, i.e., $\eta=0$ in the W-plane as shown in Fig.1. To find this transformation, we first use $T=Z/r$ to transform the semi-circle with radius r into the semi-circle with radius 1, then use the transformation

$$W=\frac{1}{2}\left(T+\frac{1}{T}\right)=\frac{1}{2}\left(\frac{Z}{r}+\frac{1}{\frac{Z}{r}}\right) \tag{15}$$

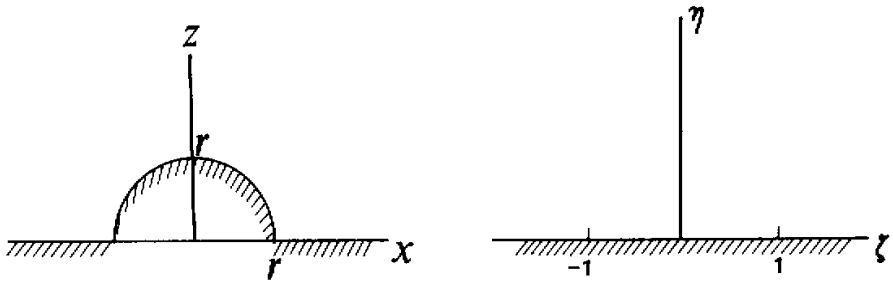

Fig.1. The conformal mapping.

to transform the semi-circle with unit radius and the real axis outside the semi-circle into the whole real axis in the W-plane. The two points $(r,0),(-r,0)$ in the Z-plane are transformed into the points $(1,0)$ and $(-1,0)$ in the W-plane respectively, the semi-circle in the Z-plane is transformed into the line segment betwwen -1 and 1 in the W-plane, the line segments between $(r,0)$ and $(\infty,0)$, $(-r,0)$ and $(-\infty,0)$ in the Z-plane are transformed into the line segments between $(1,0)$ and $(\infty,0)$, $(-1,0)$ and $(-\infty,0)$ respectively, the point $(0,r)$ in the Z-plane becomes the origin in the W-plane. The Eq.(11) in the W-plane becomes:

$$\frac{\partial^2\theta}{\partial\zeta^2}+\frac{\partial^2\theta}{\partial\eta^2}=\left\{\left.\frac{d^2F(x)}{dx^2}\right|_{xe^{\alpha t}}\cdot\frac{1}{\left|\frac{d\Phi}{dZ}\right|^2}\right\}_{\text{(16)}}$$

where $x=\varphi_1(\zeta,\eta)$, $y=\varphi_2(\zeta,\eta)$ mean that the x,z in (16) are expressed through ζ,η by the reverse transformation:

$$Z=\Phi_1(w) \tag{17}$$

Because the lower boundary in the W-plane has become the straight line, so that the condition (12) may be written as:

$$\theta(\zeta,0,t)=F[\varphi_1(\zeta,\eta)_{\eta=0}e^{\alpha t}]+\frac{1}{\varepsilon}[h(xe^{\alpha t},0)-h(x,t)]_{x=\varphi_1(\zeta,\eta)_{\eta=0}}$$

$$\text{where}\qquad \eta=0 \tag{18}$$

The upper and lateral boundary conditions still are:

$$\theta \text{ is finite} \qquad \text{where } \eta\to\infty,\ |\zeta|\to\infty \tag{19}$$

Now the problem is to solve Eq.(16) under the conditions (18),(19). Setting the r.h.s. of Eq.(16) as $\Omega(\zeta,\eta)$, we have the solution of Poisson equation (16)

$$\theta(\zeta,\eta)=\frac{\eta}{\pi}\int_{-\infty}^{\infty}\frac{F[\varphi_1(\lambda,0)e^{\alpha t}]+[\frac{1}{\varepsilon}h(xe^{\alpha t},0)-\frac{1}{\varepsilon}h(x,t)]_{x=\varphi_1(\lambda,0)}}{(\lambda-\zeta)^2+\eta^2}d\lambda$$
$$+\frac{1}{4\pi}\int_0^{\infty}d\sigma\int_{-\infty}^{\infty}d\lambda\Omega(\lambda,\sigma)\ln\frac{(\lambda-\zeta)^2+(\sigma-\eta)^2}{(\lambda-\zeta)^2+(\sigma+\eta)^2} \tag{20}$$

The solution in the Z-plane may be found through expressing the ζ, η in Eq.(20) in terms of x, z by means of (14). As an example, assuming $r=0.25$, we have $T=4Z$, Eq.(14) becomes:

$$\zeta=\frac{1}{2}[4x+\frac{x}{4(x^2+z^2)}],\qquad \eta=\frac{1}{2}[4z-\frac{z}{4(x^2+z^2)}] \tag{21}$$

In order to find $x=\varphi_1(\zeta,\eta)$, $z=\varphi_2(\zeta,\eta)$, first we find Z from (15), then obtain x and z:

$$x=r\left\{\zeta\pm\frac{1}{2}\sqrt{2[\sqrt{(\zeta^2+\eta^2-1)^2+4\zeta^2\eta^2}+(\zeta^2-\eta^2-1)]}\right\}=\varphi_1(\zeta,\eta) \tag{22}$$

$$z=r\left\{\eta\pm\frac{1}{2}\sqrt{2[\sqrt{(\zeta^2+\eta^2-1)^2+4\zeta^2\eta^2}-(\zeta^2-\eta^2-1)]}\right\}=\varphi_2(\zeta,\eta) \tag{23}$$

if $\zeta>0$, positive signs are chosen both in (22) and (23), when $\zeta<0$, negative and positive signs are taken in φ_1 and φ_2 respectively, $\left|\frac{d\Phi}{dZ}\right|^2$ in (16) may be found from (15):

$$\left|\frac{d\Phi}{dZ}\right|^2=4\left[\frac{(x^2+z^2)^2}{(x^2+z^2)^2-2(x^2-z^2)+1}\right]r^2$$

which can be expressed in terms of ζ, η by (22) and (23).

III. COMPUTATIONAL PROCEDURE AND THE EXTENSION OF THE MODEL

We shall discuss the computation of the integral (20), as an example, similar to Bannon (1983), assume:

$$F(x)=\frac{2}{\pi}\operatorname{arctg}x$$

The integral of the term containing F in the first integral in (20) may be written as:

$$\begin{aligned}
S_1&=\frac{\eta}{\pi}\int_{-\infty}^{\infty}F\frac{[\varphi_1(\lambda,0)e^{\alpha t}]}{(\lambda-\zeta)^2+\eta^2}d\lambda=\frac{\eta}{\pi}\left[\int_{-\infty}^{-1}(\ )d\lambda+\int_{-1}^{0}(\ )d\alpha+\int_{0}^{1}(\ )d\lambda+\int_{1}^{\infty}(\ )d\lambda\right]\\
&=\frac{\eta}{\pi}\int_{-\infty}^{-1}\frac{2}{\pi}\frac{\operatorname{arctg}[(\lambda-\sqrt{\lambda^2-1})re^{\alpha t}]}{(\lambda-\zeta)^2+\eta^2}d\lambda+\frac{\eta}{\pi}\int_{-1}^{0}\frac{2}{\pi}\frac{\operatorname{arctg}(r\lambda e^{\alpha t})}{(\lambda-\zeta)^2+\eta^2}d\lambda\\
&\quad+\frac{\eta}{\pi}\int_{0}^{1}\frac{2}{\pi}\frac{\operatorname{arctg}(re^{\alpha t})}{(\lambda-\zeta)^2+\eta^2}d\lambda+\frac{\eta}{\pi}\int_{-1}^{\infty}\frac{2}{\pi}\frac{\operatorname{arctg}[(\lambda+\sqrt{\lambda^2-1})re^{\alpha t}]}{(\lambda-\zeta)^2+\eta^2}d\lambda\\
&=\frac{\eta}{\pi}\left\{-\int_{1}^{\infty}\frac{2}{\pi}\frac{\operatorname{arctg}[(\lambda+\sqrt{\lambda^2-1})e^{\alpha t}r]}{(\lambda+\zeta)^2+\eta^2}d\lambda+\int_{1}^{\infty}\frac{2}{\pi}\frac{\operatorname{arctg}[(\lambda+\sqrt{\lambda^2-1})e^{\alpha t}r]}{(\lambda-\zeta)^2+\eta^2}d\lambda\right.\\
&\quad\left.-\frac{2}{\pi}\int_{0}^{1}\frac{\operatorname{arctg}(\lambda e^{\alpha t}r)}{(\lambda+\zeta)^2+\eta^2}d\lambda+\int_{0}^{1}\frac{2}{\pi}\frac{\operatorname{arctg}[(\lambda e^{\alpha t}r)}{(\lambda-\zeta)^2+\eta^2}d\lambda\right\}\\
&=\frac{\eta}{\pi}\left\{\frac{2}{\pi}\int_{1}^{\infty}\operatorname{arctg}[(\lambda+\sqrt{\lambda^2-1})e^{\alpha t}r]\left[\frac{1}{(\lambda-\zeta)^2+\eta^2}-\frac{1}{(\lambda+\zeta)^2+\eta^2}\right]d\lambda\right.\\
&\quad\left.+\frac{2}{\pi}\int_{0}^{1}\operatorname{arctg}(\lambda e^{\alpha t}r)\left[\frac{1}{(\lambda-\zeta)^2+\eta^2}-\frac{1}{(\lambda+\zeta)^2+\eta^2}\right]d\lambda\right\}
\end{aligned}\tag{24}$$

The integral of the term containing h in the first integral of (20) may be computated as follows: because $h(xe^{\alpha t},0)/\varepsilon$ is not zero only in the interval $|x| \leqslant \frac{0.25}{e^{\alpha t}}$, hence the integration interval for the function $h(xe^{\alpha t},0)/\varepsilon$ in the W–plane is $|\zeta| = \frac{0.25}{e^{\alpha t}}\frac{1}{r} = \frac{1}{e^{\alpha t}} < 1$, consequently, the integration interval for $h(x,t)$ term is between $\zeta = \pm 1$, then the integral of the term containing h may be written:

$$S_2 = \frac{\eta}{\pi}\int_{-e^{-\alpha t}}^{e^{-\alpha t}} \frac{\frac{1}{\varepsilon}\sqrt{r^2-(r\lambda)^2 e^{\alpha t}}}{(\lambda-\zeta)^2+\eta^2}d\lambda - \frac{\eta}{\pi}\int_{-1}^{1}\frac{\frac{1}{\varepsilon}\sqrt{r^2-(\lambda r)^2}}{(\lambda-\zeta)^2+\eta^2}d\lambda \tag{25}$$

Obviously, the integrals (24), (25) only can be computated numerically. In order to compute the integral with infinite limit, we set $\lambda = \frac{1}{\xi}$. (24) becomes:

$$S_1 = \frac{\eta}{\pi}\left\{\frac{2}{\pi}\int_0^1 \operatorname{arctg}\left[\left(\frac{1}{\xi}+\sqrt{\frac{1}{\xi^2}-1}\right)e^{\alpha t}r\right]\left[\frac{1}{(1-\xi\zeta)^2+\eta^2\xi^2}-\frac{1}{(1+\xi\zeta)^2+\eta^2\xi^2}\right]d\xi\right.$$
$$\left.+\frac{2}{\pi}\int_0^1 \operatorname{arctg}(\lambda e^{\alpha t}r)\left[\frac{1}{(\lambda-\zeta)^2+\eta^2}-\frac{1}{(\lambda+\zeta)^2+\eta^2}\right]d\lambda\right\} \tag{26}$$

The double integral S_3 in (20) is computed as follows, because

$$\Omega = \frac{2}{\pi}\left.\frac{(-2e^{\alpha t}x)}{(1+x^2e^{2\alpha t})^2}\right|_{x=\varphi_1(\lambda,\sigma)} \cdot 4r^2\left[\frac{(x^2+z^2)^2}{(x^2-z^2)^2-2(x^2-z^2)+1}\right]_{\text{conjugate}}$$

we have

$$S_3 = \frac{1}{4\pi}\int_0^\infty d\sigma\int_{-\infty}^{\infty} d\lambda\Omega\ln\frac{(\lambda-\zeta)^2+(\sigma-\eta)^2}{(\lambda-\zeta)^2+(\sigma+\eta)^2} = \frac{1}{4\pi}\int_0^\infty d\sigma\left[\int_{-\infty}^{0}(\,)d\lambda+\int_0^\infty(\,)d\lambda\right] \tag{27}$$

the x, z in Ω should be substituted by λ, σ according to (22), (23), this yields:

$$S_3 = \frac{1}{4\pi}\int_0^\infty d\sigma\left(\int_0^\infty d\lambda\Omega_1\ln\frac{(\lambda+\zeta)^2+(\sigma-\eta)^2}{(\lambda+\zeta)^2+(\sigma+\eta)^2}+\int_0^\infty d\lambda\Omega\ln\frac{(\lambda-\zeta)^2+(\sigma-\eta)^2}{(\lambda-\zeta)^2+(\sigma+\eta)^2}\right)$$
$$= \frac{1}{4\pi}\int_0^\infty d\sigma\int_0^\infty d\lambda\Omega_1\ln\frac{[(\lambda+\zeta)^2+(\sigma-\eta)^2][(\lambda-\zeta)^2+(\sigma+\eta)^2]}{[(\lambda+\zeta)^2+(\sigma+\eta)^2][(\lambda-\zeta)^2+(\sigma-\eta)^2]} \tag{28}$$

where $\Omega_1 = -\Omega$, putting $\zeta = \lambda$, $S^{-1} = \sigma$, we may rewrite (28) as:

$$S_3 = \frac{1}{4\pi}\left(\int_0^1 d\sigma\int_0^\infty(\,)d\lambda+\int_1^\infty d\sigma\int_0^\infty(\,)d\lambda\right) = \frac{1}{4\pi}\left(\iint_0^1 d\sigma_0^1(\,)d\lambda+\int_0^1 d\sigma\int_1^\infty(\,)d\lambda\right.$$
$$\left.+\int_1^\infty d\sigma+\int_0^1(\,)d\lambda+\int_1^\infty d\sigma\int_1^\infty(\,)d\lambda\right)$$
$$= \frac{1}{4\pi}\left[\int_0^1 d\sigma\int_0^1 d\lambda\Omega_1\ln\frac{[(\lambda+\zeta)^2+(\sigma-\eta)^2][(\lambda-\zeta)^2+(\sigma+\eta)^2]}{[(\lambda+\zeta)^2+(\sigma+\eta)^2][(\lambda-\zeta)^2+(\sigma-\eta)^2]}\right.$$

$$+\int_0^1 d\sigma\int_0^1 d\xi\frac{\Omega_1}{\xi^2}\ln\left\{\frac{[(1+\zeta\xi)^2+(\sigma-\eta)^2\xi^2]}{[(1+\lambda\xi)^2+(\sigma+\eta)^2\xi^2]}\times\frac{[(1-\zeta\xi)^2+(\sigma+\eta)^2\xi^2]}{[(1-\zeta\xi)^2+(\sigma-\eta)^2\xi^2]}\right\}$$

$$\int+\int_0^1 d\lambda\int_0^1\frac{ds}{s^2}\ln\left\{\frac{[s^2(\lambda+\zeta)^2+(1-\eta t)^2][s^2(\lambda-\zeta)^2+(1+\eta s)^2]}{[s^2(\lambda+\zeta)^2+(1+\eta t)^2][s^2(\lambda-\zeta)^2+(1-\eta s)^2]}\right\}\Omega_1$$

$$+\int_0^1 d\zeta\int_0^1\frac{d\xi}{s^2\xi^2}\Omega_1\ln\left\{\frac{[s^2(1+\zeta\xi)^2+(1-\eta s)^2\xi^2][s^2(1-\zeta\xi)^2+(1+s\eta)\xi^2]}{[s^2(1+\zeta\xi)^2+(1+\eta s)^2\xi^2][s^2(1-\zeta\xi)^2+(1-s\eta)^2\xi^2]}\right\}\Bigg] \tag{29}$$

The summation of (25),(26),(29) is the solution of Eq.(16) in the W–plane, the solution in the Z–plane can be found through expressing ζ, η in terms of x, z according to (21). The integrals in the above formulas may be computed numerically using Simpson formula. It is not difficult to prove that the individual singular points in the integrals do not affect the existence and convergence of these integrals.

The θ field is thus obtained, adding the basic state potential temperature (assuming $\Theta_0 = 280$ K at $z=0$), we get total potential temperature $\Theta=\Theta_0\left(1+\varepsilon\frac{fl^2}{gD}\theta\right)$ (Pedlosky, 1979). After θ is computed, we can calculate $w_1=-\left(\frac{\partial\theta}{\partial t}-\alpha x\frac{\partial\theta}{\partial x}\right)$ from (5), and the divergence of the ageostrophic wind from $\frac{\partial u_1}{\partial x}=-\frac{\partial w_1}{\partial z}$ (using the finite difference analog).

We have solved the problem for which the center of the mountain is located at the center of the deformation field, if the center of the mountain is located at $x=a$, which is not the center of the deformation field, we can see that the lower boundary $z=h$ will take a new form but the equation and the lower boundary condition do not change. In order to apply conformmapping, we first use the transformation $T_1=Z-a$ to transform the center of the mountain from $x=a$ to the origin, then use the above conformal mapping, hence,

$$W=\frac{1}{2}\left(\frac{Z-a}{r}+\frac{1}{\frac{Z-a}{r}}\right) \tag{30}$$

i.e.,

$$\zeta=\frac{1}{2}\left[\frac{x-a}{r}+\frac{r(x-a)}{(x-a)^2+z^2}\right] \tag{31}$$

$$\eta=\frac{1}{2}\left[\frac{z}{r}-\frac{rz}{(x-a)^2+z^2}\right] \tag{32}$$

x and z can be found from (30) as:

$$x=r\left[\zeta\pm\frac{1}{2}\sqrt{2[\sqrt{(\zeta^2+\eta^2-1)^2+4\zeta^2\eta^2}+(\zeta^2-\eta^2-1)]}\right]+a \tag{33}$$

$$z=r\left[\eta\pm\frac{1}{2}\sqrt{2[\sqrt{(\zeta^2+\eta^2-1)^2+4\zeta^2\eta^2}-(\zeta^2-\eta^2-1)]}\right] \tag{23}$$

The procedure for solving the Poisson equation is similar to that when the mountain is located at the center of the deformation field, but the integration (25) should be changed, in this case, $h=\sqrt{r^2-(x-a)^2}$ for $|x-a|\leqslant r$, and $h=0$ at other x, the integration should be altered correspondently.

We have discussed the situation that the mountain is motionless with respect to the deformation field, next, we shall discuss the mountain removing with respect to the deformation field. Similar to Bannon (1983), we assume that the deformation field is motionless but the mountain removes, we solve the problem in the coordinate system at the time t. In the Z–plane, the origin is assumed to be located at the center of the static deformation field. The coordinate of the mountain center is $x = a$ at $t = 0$ but $x = a_1$ at time t, in this case, according to (9), the lower boundary condition should be:

$$\theta(x,h,t) = \theta(x,h_0,0) + \frac{1}{\varepsilon}\left[h_0(xe^{\alpha t},0) - h(x,t)\right] \tag{34}$$

where subscript 0 represents the value corresponding to the mountain shape at $t = 0$ because the shapes of the lower boundary are different at different times. On the lower boundary at $t \neq 0$, the boundary condition should be:

$$\theta = F(xe^{\alpha t},h_0,0) + \frac{1}{\varepsilon}\left[h_0(xe^{\alpha t},0) - h(x,t)\right] \tag{35}$$

We apply the conformal mapping at time t, transform the mountain with the center at a_1 and the real axis outside the mountain in the Z–plane into the real axis in the W–plane and the point (a_1,r) is transformed into origin, in this new W–plane, we can solve the problem with above mentioned method, the lower boundary condition at time t may be easily expressed in the W–plane, in this case, h_0 should be the topography at $t = 0$ in the coordinate system at time t.

For example, as have been described, the location of the mountain center is $x = a$ at $t = 0$ but $x = a_1$ at time t in the Z–plane, assuming that the mountain shapes at these two times do not overlap each other. At time $t = 0$ in the Z–plane, the mountain shape in the coordinate system for which the origin is located at the center of the deformation field is:

$$\begin{aligned} &h_0 = \sqrt{r^2 - (x-a)^2} && \text{where} \quad -r < x - a < r \\ &h_0 = 0 && \text{for other} \quad x \end{aligned}$$

At time t, in the W–plane for which the mountain peak in the Z–plane is transformed into the origin,

$$\begin{cases} h_0(xe^{\alpha t},0) = \sqrt{r^2 - \{[r(\zeta \pm \sqrt{\zeta^2 - 1}) + a_1]e^{\alpha t} - a\}^2} \\ h_0(xe^{\alpha t},0) = 0 \qquad \text{for other } \zeta \\ \text{where} \quad -r < [r(\zeta \pm \sqrt{\zeta^2 - 1}) + a_1]e^{\alpha t} - a < r \end{cases} \tag{36}$$

$$\begin{cases} h(x,t) = \sqrt{r^2 - (r\zeta)^2} & \text{where} \quad |\zeta| \leqslant 1 \\ h(x,t) = 0 & \text{for other} \quad \zeta \end{cases} \tag{37}$$

Eq.(29) needn't to be changed because it is independent of the lower boundary condition, but (24),(25) must be changed. The lower boundary condition (35) is linear, so that the solution corresponding to (35) may be taken as the summation of the solutions when the each term in (35) appears separately. The solution corresponding to the first term of (35) is (see (24)):

$$\theta_1 = \frac{\eta}{\pi}\left\{\int_{-\infty}^{-1} \frac{2}{\pi}\frac{\operatorname{arctg}\{[r(\lambda - \sqrt{\lambda^2 - 1}) + a]e^{\alpha t}\}}{(\lambda - \zeta)^2 + \eta^2}\,d\lambda + \int_{-1}^{0} \frac{2}{\pi}\frac{\operatorname{arctg}\{e^{\alpha t}(r\lambda + a)\}}{(\lambda - \zeta)^2 + \eta^2}\,d\lambda\right.$$

$$+\int_0^1 \frac{2}{\pi}\frac{\operatorname{arctg}\{(r\lambda+a)e^{\alpha t}\}}{(\lambda-\zeta)^2+\eta^2}d\lambda+\int_1^{\infty}\frac{2}{\pi}\frac{\operatorname{arctg}\{e^{\alpha t}[r(\lambda+\sqrt{\lambda^2-1})+a]\}}{(\lambda-\zeta)^2+\eta^2}d\lambda \tag{38}$$

with preceding transformation, $\int_{-\infty}^{-1}$ can be changed into $\int_0^1$ and $\int_{-1}^{0}$ into $\int_0^1$. The solution corresponding to the second and third terms of (35) is:

$$\theta_2=\frac{\eta}{\pi}\int_{\zeta_{\min}}^{\zeta_{\max}}\frac{\frac{1}{\varepsilon}\sqrt{r^2-\{[r(\lambda\pm\sqrt{\lambda^2-1})+a_1]e^{\alpha t}-a\}^2}}{(\lambda-\zeta)^2+\eta^2}d\lambda$$
$$-\frac{\eta}{\pi}\int_{\zeta'_{\min}}^{\zeta'_{\max}}\frac{\frac{1}{\varepsilon}\sqrt{r^2-(r\lambda)^2}}{(\lambda-\zeta)^2+\eta^2}d\lambda \tag{39}$$

where $\zeta_{\min}$, $\zeta_{\max}$, $\zeta'_{\min}$ and $\zeta'_{\max}$ are the upper and lower limits of ζ which corresponds to the non-zero value of h. The solution of θ should be the summation of θ_1, θ_2 and (29). The solution for the removing mountain is thus derived.

IV. THE RESULTS IN CASE THAT THE MOUNTAIN IS LOCATED AT THE CENTER OF DEFORMATION FIELD

We analyse the frontogenesis at different times from the isoline of Θ. At $t=0$, the Θ isolines should be the horizontal straight lines. Fig.2 depicts the Θ isoline at $\alpha t=2$ without the topography, the basic state Θ at ground level is assumed to be 280 K. It is seen that the isolines are concentrated obviously at the lower levels of the central part of the deformation field, i.e., the frontogenesis phenomenon occurs there. Fig.3 depicts the Θ isolines in case that the mountain is located at the center of the deformation field. It can be seen that at the level corresponding to the mountain level, the $|\nabla\theta|$ on the r.h.s. of the figure (i.e., the warm

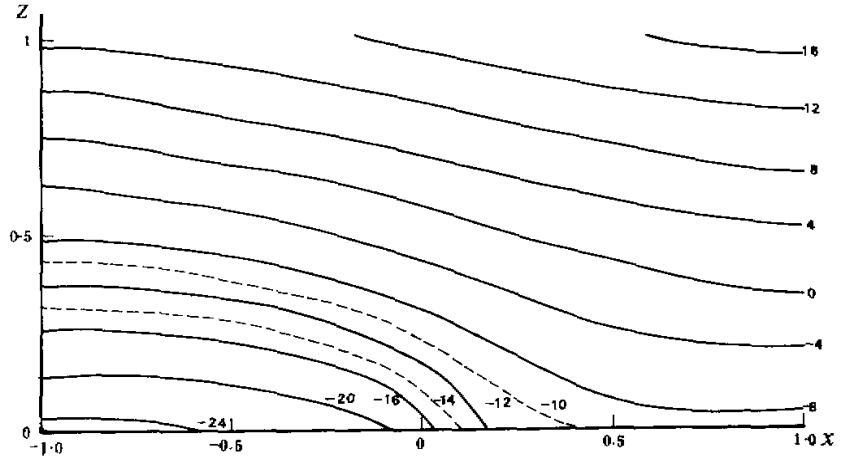

Fig.2. The Θ isolines above flat ground at $\alpha t=2$, the interval of the isolins is 4 K, near the mountain the interval is doubled, the values in this figure correspond to the real value subtracting 300 K.

sector) is stronger than that over flat ground and the reverse is true for the l.h.s., in other words, the warm front will strengthen and the cold front will weaken in the upslope side, it is in agreement with Bannon's results. It can be explained from (18), because the mountain is higher in the central part , it makes the effect of $h(x,t)$ be greater than that of $h(xe^{\alpha t},0)$, this means that the effect of the topography in the lower boundary condition is the cooling caused by the forced ascending motion due to the topography (Bannon,1983), which results in that the potential temperatures of the mountain surface and over the mountain will be lower than that at the same level in case of flat ground, this makes the vertical gradient of the potential temperature over the mountain increase, i.e., the static stability will be greater than that over the flat ground.

In the horizontal direction, because air over the mountain is cooler, the $|\nabla\theta|$ to the r.h.s. will be greater, this results in that the r.h.s. of the mountain is of advantage to frontogenesis and the l.h.s. is of advantage to frontolysis. Bannon (1983)'s work only can obtain the characteristics of the frontogenesis and frontolysis at the level of the mountain on account of his treatment on the lower boundary condition. In this paper, the frontogenesis and frontolysis characteristics not only at the mountain height but also on the mountain slopes are demonstrated. It is shown that on the mountain slope, the frontogenesis and frontolysis phenomena are more remarkable than that at the mountain peak level. From the Θ isolines it can be seen that the frontogenetical areas are located on the warm side and peak of the mountain. Far away the mountain, the frontogenesis phenomenon is not notable. From the distributions of $\partial\theta/\partial x$ and frontogenesis function $\frac{d}{dt}\nabla\theta = -\frac{\partial u}{\partial x}\frac{\partial\theta}{\partial x} - \frac{\partial w}{\partial x}\frac{\partial\theta}{\partial z}$ in the vertical cross section (Fig.4), it can be seen that the main frontogenetical area is located at the mountain slope in the warm sector and mountain peak, the frontolytical area is located at the slope of the cold sector.

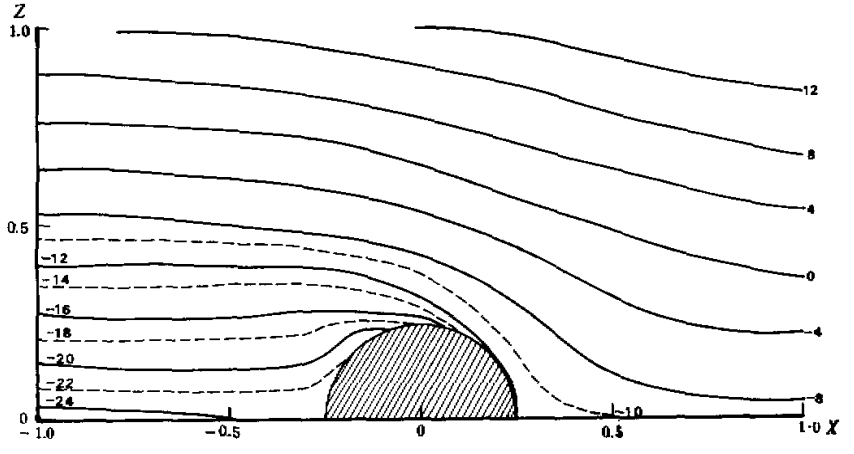

Fig.3. The Θ isolines at $\alpha t = 2$ in case that the mountain is located at the center of the deformation field.

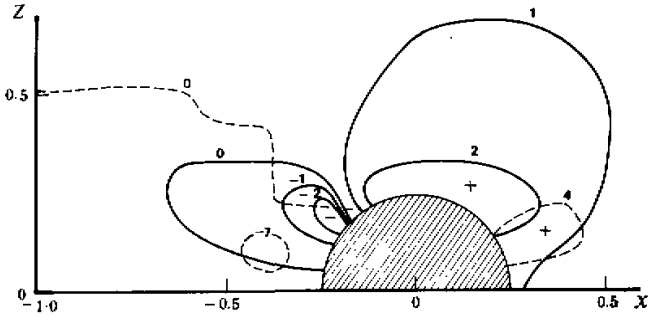

Fig.4. The distributions of $\partial\theta / \partial x$ and frontogenesis function when the mountain is located at the center of the deformation field, solid line is for $\partial\theta / \partial x$, dashed line is for frontogenesis function.

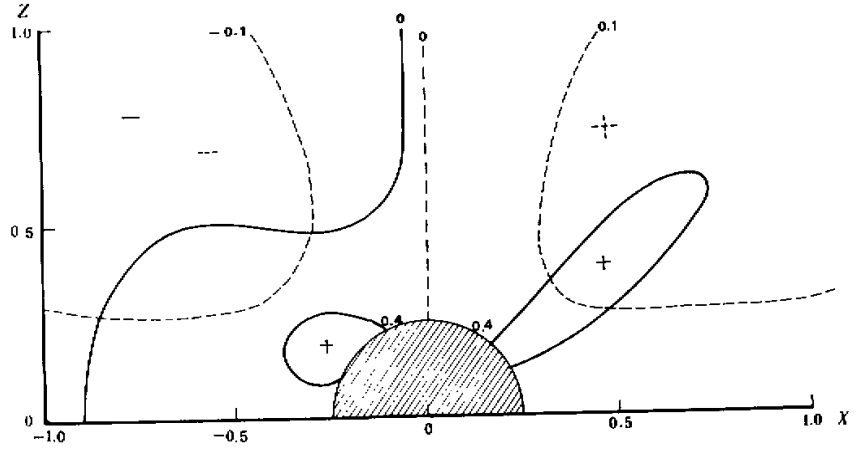

Fig.5. The vertical velocity distribution in case of flat ground and when the mountain is located at the center, dashed line represents w_1 in case of flat ground, solid line is for w_1 in case of mountain.

The vertical velocity w_1 is depicted in Fig.5, which shows there are ascending motion in the warm sector and descending motion in the cold sector, which are caused by the deformation field, similar to Bannon's results, but there exists an ascending motion region

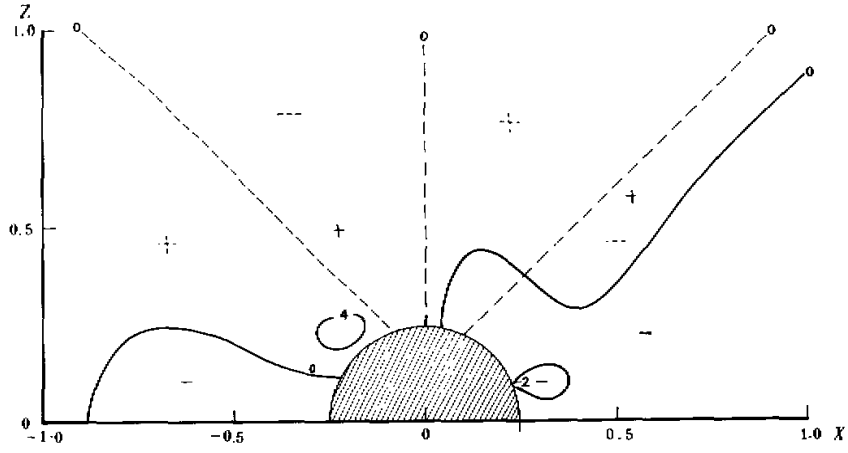

Fig.6. The divergence field when the mountain is located at the center and in case of the flat ground, dashed line represents the zero isoline of divergence in case of the flat ground.

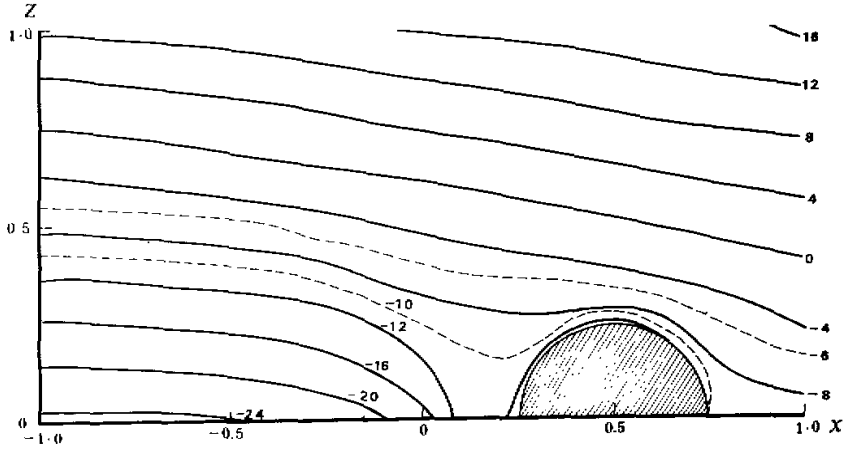

Fig.7. The Θ distribution when the mountain is located on the r.h.s. of the deformation field.

near the mountain in cold sector caused by climbing mountain process. The ascending motion in the warm sector is also located on the slope with the same cause as that in the cold sector. The dashed line in Fig.5 represents the vertical velocity in case of flat ground. The difference between the solid and dashed lines shows the remarkable dynamic effect of the topography.

Fig.6 displays the divergence field due to ageostrophic wind. Convergence is present on the two sides of the center near the surface, divergence distributes over all other places. In comparing with the case of the flat ground, we can see that when the topography is not included, there is convergence in the lower part and divergence aloft in the warm sector, the reverse is true in the cold sector. When the topography is considered, convergence is present on the two sides of the center below the mountain level which is also caused by the dynamical effect of the topography, i.e., the blocking effect of the mountain causes deceleration and convergence. Because convergence is present in the lower part of cold sector which makes divergence aloft, so that the divergence field in the cold sector is just reverse to that over the flat ground. In summary, below the level of the mountain peak, both sides of the mountain there exists $\partial u_1 / \partial x < 0$, i.e., the mountain plays the blocking role on air flow and the moving speed of the front.

V. THE RESULTS WHEN THE MOUNTAIN IS NOT LOCATED AT THE CENTER OF THE DEFORMATION FIELD

Assuming the center of the mountain to be located at $a = 0.5$, i.e., on the r.h.s. of the deformation field, it is not difficult to obtain the solution by using the coordinate transformation in Section III. Fig.7 displays the Θ distribution at $\alpha t = 2$. Comparing with Fig.1 for the case of the flat ground, the similar phenomenon appears like the case when the mountain is located at the center, near the peak, the decrease of the Θ is equivalent to raising the Θ isolines, hence, at the peak level, $|\nabla\theta|$ between the mountain and warm air on the r.h.s. will increase, the reverse is true between the mountain and cold air on the left.

At $z = 0$, the result is more complicated, in case of the flat ground, there is frontogenesis at $z = 0$ level near the origin, but when the mountain is located on the r.h.s. of the deformation field, the potential temperature will increase at the surface level between the mountain and the center of the deformation field on account of the role of the term $h(xe^{\alpha t}, 0)$ in Eq.(18) (i.e. Bannon's "warm anomaly"), this will strengthen the gradient of θ between this region and cold air on the l.h.s. of the deformation field, in other words, $|\nabla\theta|$ will be greater near the origin. In summary, under this relative location of the topography with respect to the deformation field, on the left of the mountain, frontogenesis will occur at the level of the mountain peak, but there will be frontolysis between the warm and cold air at the surface level. On the other hand, the above mentioned increase of θ at the surface level will make the $|\nabla\theta|$ in the space to the mountain body decrease.

The topography characteristics of the above discussed cases are that the mountain is located at the warm part of the deformation field, in this case, in general, there will be of advantage to frontogenesis upstream of the mountain and frontolysis downstream of the mountain for the warm front, at the same time, the frontogenesis characteristics on the slope and surface will be more complicated. $\partial\theta / \partial x$ and $\frac{d}{dt}\nabla\theta$ are also have similar characteristics. Although the mountain is assumed to be motionless with respect to the deformation field here, but the conclusion is in agreement with Bannon's (1983) that it is of advantage to the frontogenesis in front of the mountain and to the frontolysis behind the mountain for warm front, even Bannon's conclusion is for the moving warm front. Our results are finer than Bannon's over the slope and flat terrain.

The w_1 distribution is shown in Fig.8. $w_1 < 0$ on the l.h.s. of the figure retains the characteristics over the flat ground, on the r.h.s. of the figure, there appears ascending motion on the right and descending motion on the left of the mountain on account of

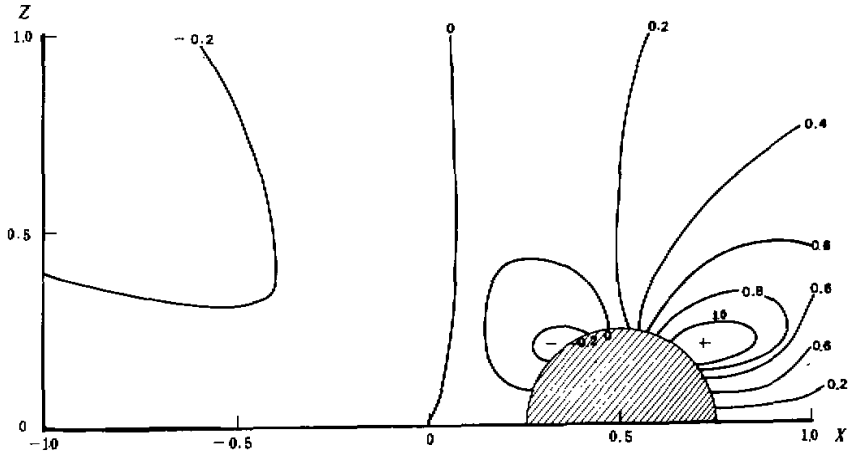

Fig.8. The w_1 distribution when the mountain is located on the right of the deformation field.

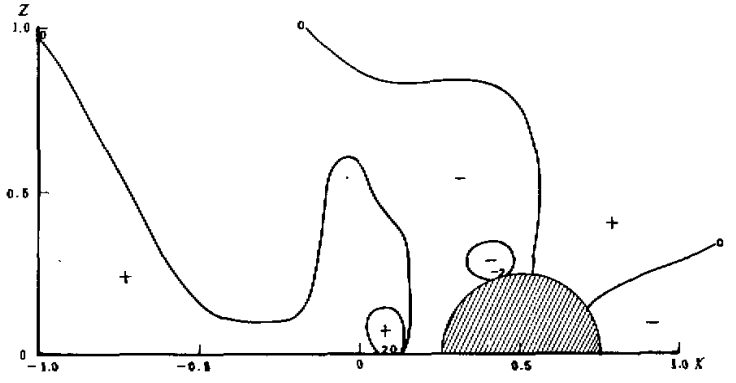

Fig.9. The divergence field when the mountain is located on the right of the deformation field.

the forced effect of the mountain, the importance of the force by the topography can be seen. For the staticstability, it increases over the mountain peak, but decreases on the two sides of the mountain as before. The divergence field is depicted in Fig.9, it retains basically the characteristics thatthe convergence and divergence are present in the lower and upper parts of the warm sector respectively and vice versa for the cold sector, except that, there appear divergence and convergence in the lower and upper parts respectively between the mountain and the center of the deformation field, which is caused by downslope motion on the left of the mountain.

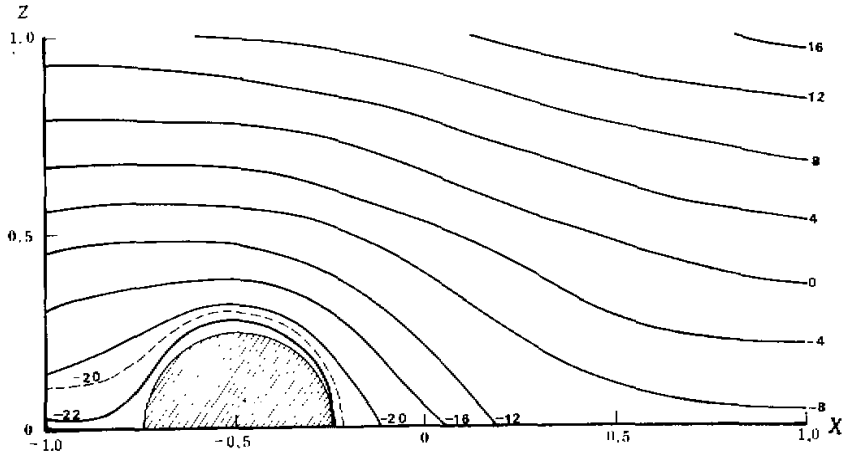

Fig.10. The Θ distribution when the mountain is on the left of the mountain.

Fig.10 demonstrates the Θ field at $\alpha t = 2$ when the mountain center is located at $a = -0.5$, the left part of the deformation field. The distribution is just reverse to that when $a = 0.5$ because the Θ decreases on the level of the mountain height. The $|\nabla\theta|$ to the warm air on the right side increases, that to the cold air on the left decreases, even $\nabla\theta$ changes the sign. For the level of the flat ground behind the mountain, on account of the small increase of temperature caused by the "warm anomaly", the gradient of temperature to the warm sector is both smaller than that at the mountain level and that in case of flat terrain (Fig.1), i.e., on the flat ground behind the mountain the frontogenesis effect to the warm air will decrease.

As for the w_1 distribution, the ascending motion retains in the warm sector due to the absence of the mountain, in the cold sector, a positive center appears in front of the mountain due to the climbing mountain movement as Fig.11, in contrast with the descending motion in case of flat terrain. For $\partial u_1 / \partial x$, there still are convergence in the lower and divergence in the upper parts in the warm sector, but for the cold sector, the convergence in the lower and divergence in the upper parts in front of the mountain appear in contrast with the divergence in the lower and convergence in the upper parts over the flat terrain. Obviously, this is caused by the retardation effect of the topography.

Next we shall consider the case of moving mountain, assuming $a = 0.5$ at $t \to 0$, but the mountain removes to the $a = -0.5$ at $\alpha t = 2$, the Θ distribution is displayed in Fig.12 according to (35), the temperature at the lower boundary will be affected by the reverse roles of the h at new time and the h at $t = 0$. This case corresponds to the case that the deformation field removes from the left to the right of the mountain. It should be mentioned that the method in this paper can not research the evolution of a mature front across the mountain, because at $t = 0$ the Θ isolines still are flat, the frontogenesis occurs gradually only in the removing process of the deformation field with respect to the mountain, i.e., the method in this paper only can investigate the effect of the mountain on the forming condition of the front. Comparing with Fig.1, at $\alpha t = 2$, the decreasing of the temperature over the mountain causes the $|\nabla\theta|$ to increase on the r.h.s. of the mountain and vice cersa on the

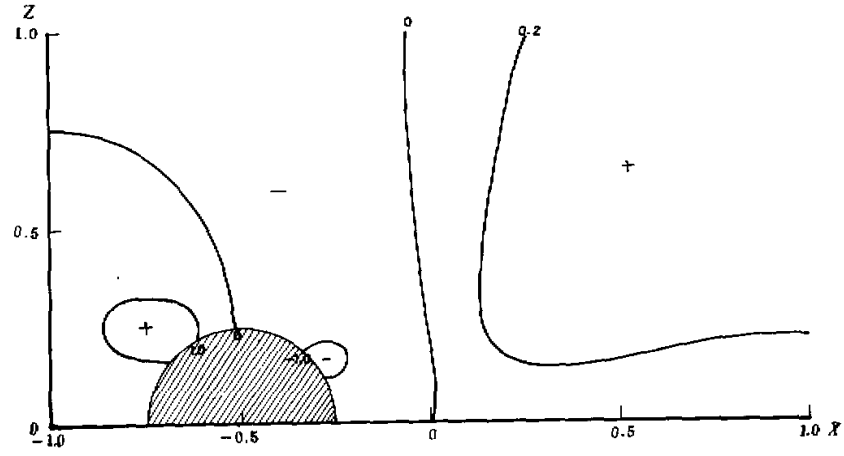

Fig.11. The W_1 distribution when the mountain is located on the left of the deformation field.

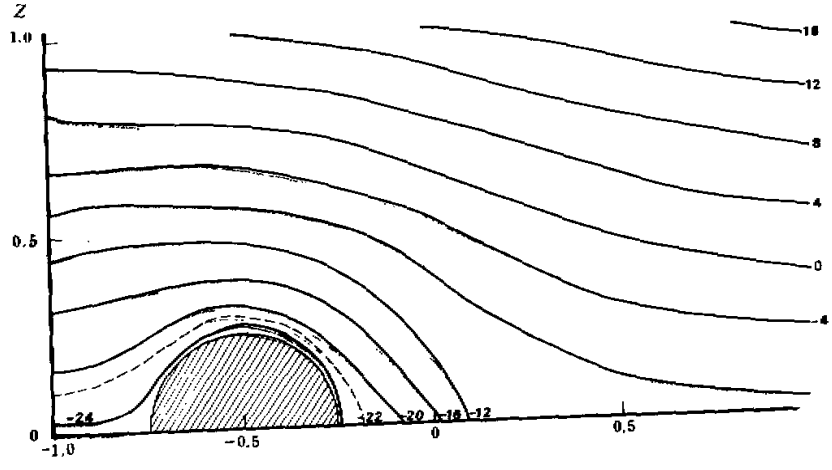

Fig.12. The Θ distribution when the mountain removes from $a = 0.5$ to $a = -0.5$.

l.h.s., therefore, the conclusion that the area behind the mountain is of advantage to th frontogenesis for the cold front is again obtained. Its difference to that for the motionle

mountain in Fig.10 is that the locations of the mountain at $t = 0$ are different, on account of the effect of the mountain at $t = 0$, the difference of the temperature on the two sides of the center of the deformation field for Fig.12 is stronger than that in Fig.10, so that it is of advantage to the frontogenesis both at the level of the mountain and on the ground near the center of the deformation field.

For the case that the mountain center is located at $a = -0.5$ at $t = 0$ and $a = 0.5$ at $\alpha t = 2$, i.e., corresponds to that the deformation field removes from right to the left, the Θ distribution is similar to Fig.7 approximately except that $|\nabla\theta|$ near the center of the deformation field is weaker slightly than that in Fig.7 due to the slight increase of temperature below the level of the mountain caused by the "warm anomaly" at $t = 0$, i.e., for warm front, the frontogenetical effect is weakened near the surface behind the mountain.

VI. CONCLUSIONS

In this paper, real terrain is included for the lower boundary condition in Bannon's quasi-geostrophic frontogenesis model, the influences of the topography on the frontogenesis are obtained. We not only prove the general characteristics of the effect of the topography on the cold and warm fronts, i.e., it is of advantage to frontogenesis for the warm front and frontolysis for the cold front in front of the mountain and the reverse is true behind the mountain, but also derive the fine structures of the frontogenesis and frontolysis effects between the mountain peak and the flat ground where the characteristics of the frontogenesis and frontolysis are different from that at the mountain peak level. The characteristics also are different when the deformation field is motionless or moving, i.e., the frontogenetical characteristics depend on the moving speed of the deformation field with respect to the topography. For w_1 and divergence fields of ageostrophic wind, their characteristics reflect the summation of both the effects of the deformation field and the forced motion by the topography which shows the importance of the dynamic effect of the topography. It is noted that the conclusion of this paper is derived under the assumption that the initial potential temperature disturbance is independent of z, the actual condition may be more complex than this ideal case. Furthermore, the disturbed wind field εu_1 from the approximate result of $\partial u_1 / \partial x$ in this paper can be estimated approximately, it is shown that the disturbed wind speed usually is much less than or less than the basic wind speed except near the center of the deformation field where the basic wind speed is of the same order of magnitude as the disturbed wind, hence, the linearized method in this paper usually is available except near the center of the deformation field. Due to this disturbed wind field, the real wind field has some deviation to the ideal deformation field both when the mountain is motionless and moving, all of these affect the accuracy of this paper. But from the viewpoint of dynamics, this paper demonstrates the dynamic process of the effect of the topography on the quasi-geostrophic frontogenesis. As have been shown in the previous section, the method of this paper can only study the advantageous or disadvantageous effects of the topography in the formation process of the front, but not be used to research the variation experienced by a mature front as it moves across a mountain, which needs to be investigated by more complex models.

REFERENCES

Bannon, P. R.(1983), Quasi-geostrophic frontogenesis over topography, *J. Atmos. Sci.*, **40**: 2266-2277.

Bannon, P. R. (1984), A semi–geostrophic model of frontogenesis,*Beitr. Phys. Atmos.*, **57**: 393–409.

Hoskins, B. J. and F. P. Bretherton (1972), Atmospheric frontogenesis model: Mathematical formulation and solution, *J. Atmos. Sci.*, **29**: 11–37.

Pedlosky, J. (1979), Geophysical Fluid Dynamics, Springer Verlag.

Williams, R. and J.Plotkin (1968), Quasi–geostrophic frontogenesis, *J. Atmos. Sci.* **25**: 201–206.